Soft Zone Effects on Fatigue and Fracture of β Ti-Alloys

M. Benedetti[1,2], J. O. Peters[1] and G. Lütjering[1]

[1] Technical University Hamburg-Harburg, 21071 Hamburg, Germany
[2] University of Trento, 38050 Trento, Italy, e-mail: matteo.benedetti@ing.unitn.it

ABSTRACT. *To evaluate the effect of soft zones along β grain boundaries on crack path during fatigue crack growth and on the onset of unstable cracking (K_{Ic}) of β titanium alloys, this comparison study included large grained β annealed and β processed as well as fine grained α + β processed microstructures with extremely fine and coarse α plate sizes, and, thus, with very high ($\sigma_{0.2}$ = 1500 MPa) and low yield stress (1050 MPa). When increasing yield stress level from 1050 to 1500 MPa, basically, fatigue crack growth threshold level of ~6 MPa√m is reduced to a level of ~4 MPa√m, whereas fracture toughness values of 48 MPa√m (α + β processed) and ~70 MPa√m (β annealed or β processed) both dropped by 50 %. Differences in fatigue crack growth behavior are mainly attributed to the effect of lamellar matrix on crack front profile. While part of the increase in fracture toughness is attributed to the increase in plastic deformation of the lamellar matrix before onset of unstable crack advance occurs within the soft zones at the grain boundaries, crack growth retarding steps in the crack front lead to an increase in the ductile transgranular fracture with decreasing strength level, and, thus, also contribute to the observed increase in fracture toughness.*

INTRODUCTION

As shown in detail in a recent study [1] on the typical high strength β titanium alloy β-CEZ for large forgings, age-hardening cause the formation of continuous α layers and adjacent "soft zones" at β grain boundaries and lead to a high strength difference between the age-hardened matrix and the soft zone at β grain boundary. While in this recent study two β annealed microstructures with extremely fine and coarse α plate sizes and, thus, with very high and low strength were compared to evaluate the effect of soft zones along β grain boundary on fracture toughness, this study attempts to extend this comparison to β processed and α + β processed microstructures, as well as on crack extension upon fatigue loading.

MATERIAL AND EXPERIMENTAL PROCEDURE

The β-CEZ alloy (Ti-5.0%Al-1.9Sn-4.5Zr-3.9Mo-2.2Cr-1.1Fe-0.10 O, wt.%, β-transus: 890°C) was delivered by CEZUS, France. The β annealed high strength condition with equiaxed β grains (400 µm) was obtained by β annealing and subsequent fast cooling (600°C/min) to room temperature (Figs. 1a and 1b). Very fine incoherent α platelets were precipitated during final aging treatment at 580°C for 8 hours (TEM-Fig. 2a). In

contrast, the low strength condition (with same β grain size) was obtained by controlled cooling after β annealing with a cooling rate of 30°C/min and subsequent annealing treatment for 1 hour at 820°C followed by very slow cooling (1°C/min) in order to coarsen the α plates (Fig. 1c). The final aging treatment was identical to the first case to ensure comparability of the two conditions. The TEM-micrograph in Fig. 2b shows that slow cooling rate from annealing treatment caused no precipitation of fine incoherent α platelets during the final aging step. To change the grain shape and the grain boundary structure of the β annealed conditions a "through β-transus" forging was performed to develop a pancake shaped grain structure (Fig. 3a). After homogenization, the forging process started directly in the β phase field and was continued into the $\alpha + \beta$ phase field. However, processing parameters of this study lead to more or less continuous α layers instead of round α particles at β grain boundaries [2]. Fig. 3a shows that α layers effectively stabilize the pancake shaped β grain structure. During air cooling after the forging process α plates precipitated within the β grains. To ensure compatibility with the β annealed high strength condition, an annealing treatment at a temperature of 880°C just below the β transus (890°C) for 1 hour with subsequent fast cooling (600°C/min) was performed to reduce volume fraction of coarse α plates (Fig. 3b), and, thus, to maximize hardenability of β matrix during final aging at 580°C for 8h. For the low strength condition with pancake shaped grain structure, the annealing treatment at 820°C, the very slow cooling (1°C/min) to coarsen the lamellar matrix (Fig. 3c), and the final aging treatment were identical to the low strength β annealed condition to ensure comparability of the two microstructures. To reduce the β grain size of the β annealed conditions bimodal microstructures (Fig. 4) were obtained by conventional processing in the $\alpha + \beta$ phase field. For the high strength and low strength conditions with bimodal micostructure, the low volume fraction of the primary α and the small β grain size (40 µm) were adjusted by a recrystallization treatment at 870°C for 1 hour following the rolling process at 850 °C. Again, both bimodal conditions received the same annealing (only low strength condition) and aging treatment (both conditions) as the β annealed and the β processed microstructures to ensure comparatibility. The distribution of fine incoherent α platelets precipitated during the final aging treatment is similar for three high strength as well as for the three low strength conditions studied because of the identical final steps of annealing treatments and cooling rates. Moreover, microstructures of high strength as well as low strength conditions are characterized by more or less identical continuous α layers along the β grain boundaries as exemplarily shown for β annealed microstructures in TEM-micrographs in Fig. 2. Specifically, all high as well as all low strength conditions show continuous soft zones of non-hardened β phase adjacent to the α layers along the β grain boundaries (see arrows in Figs. 2a and 2b). The tensile properties of all conditions investigated are listed in Table 1. While the fine grained $\alpha + \beta$ processed high strength condition shows a yield stress $\sigma_{0.2}$ of nearly 1500 MPa and significant ductility (*T. E.* = 5 %), both high strength β annealed and β processed conditions failed in the linear-elastic region at a stress of ~1400 MPa, *i. e.* the yield stress $\sigma_{0.2}$ was not reached. In contrast, the low strength conditions show much lower yield stress level of ~1050 MPa and significantly higher ductility (*T. E.* ~12 %). However, testing the β processed condition in the short transverse (S-)direction resulted in a 30 %-reduction in ductility. C(T) type specimens with a thickness of 8 mm were tested to evaluate the role of soft zones on crack path during fatigue crack growth (da/dN-ΔK) and the onset of unstable cracking (K_{Ic}).

Table 1. Tensile properties and fracture toughness values of studied *b*-CEZ alloy

Microstructure	Strength condition	$s_{0.2}$ (MPa)	*UTS* (MPa)	s_F (MPa)	*T.E.* (%)	*RA* (%)	K_{Ic}, K_c (MPa m)
b annealed	high	s_0 = 1370	1370	1370	0	0	33
b processed (L)	high	s_0 = 1445	1445	1445	0	0	36 (L-T)
a+*b* annealed	high	1495	1510	1745	5	19	24
b annealed	low	1030	1110	1315	12	17	73*
b processed (L)	low	1050	1110	1385	12	23	69* (L-T)
b processed (S)	low	1060	1130	1225	8	21	57 (S-T)
a+*b* annealed	low	1060	1090	1485	15	39	48

*Fracture toughness tests did not meet thickness requirement for valid K_{Ic} values

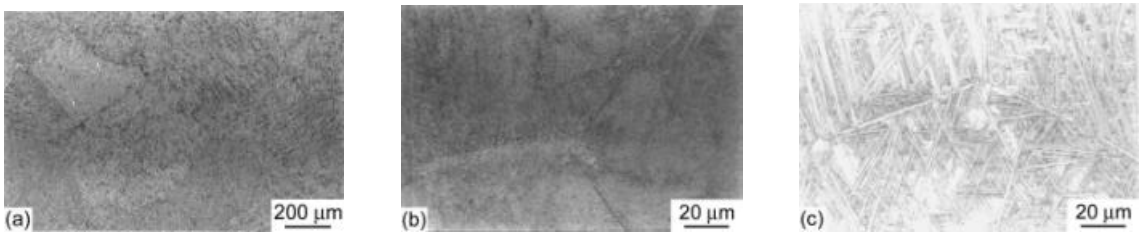

Figure 1. *b* annealed microstructures (LM). a) grain size, b) high strength c) low strength condition.

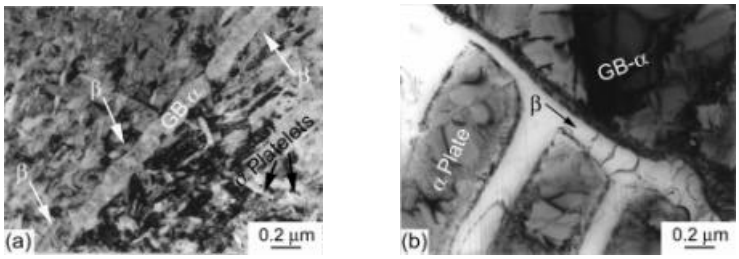

Figure 2. Lamellar matrix (*a* plates) and continuous *a* layers (GB-α) and *b* stabilized soft zones (see arrows) at *b* grain boundaries of *b* annealed microstructures (TEM). a) high , b) low strength condition.

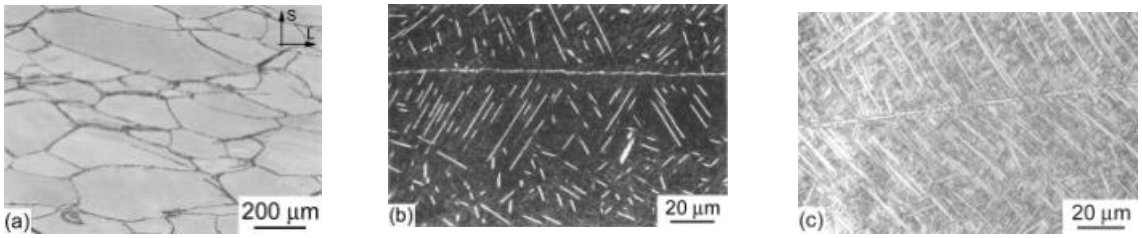

Figure 3. *b* processed pancake grain shaped microstructures (LM). a) *b* grain shape, b) high strength, c) low strength condition.

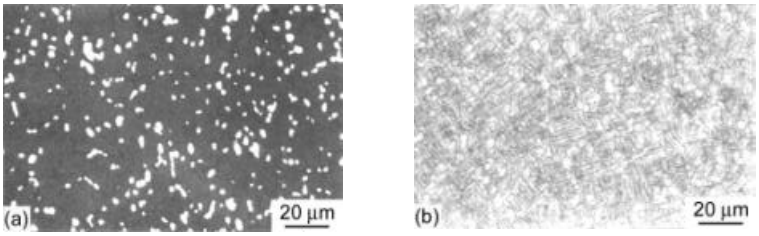

Figure 4. *a* + *b* processed bimodal microstructures (LM). a) high strength, b) low strength condition.

RESULTS AND DISCUSSION

Generally, the high yield stress level of the high strength conditions can be attributed to the small spacing between the fine incoherent ***a*** platelets (Fig. 2a) resulting in a very high resistance against dislocation movement [1]. Moreover, failure in the linear-elastic regime can be attributed to the extremely high strength difference between the matrix and the soft zone of non-hardened ***b*** phase along the continuous a layers at ***b*** grain boundaries [1,3]. Apparently, preferred plastic deformation within the soft zones is so localized that premature cracking occurs before any measurable plastic deformation of the matrix. However, the slip length for dislocation movement also contributes to premature cracking along the soft zones. As shown by fine grained bimodal condition, the short ***b*** grain boundary length reduces the effective slip length, and, thereby, leads to significant plastic deformation of the lamellar matrix before onset of unstable fracture. The reduced yield stress level of the low strength conditions effectively minimizes the strength difference between the matrix and soft zones, and, consequently, promotes significant plastic deformation of the matrix before onset of fracture within the soft zones (*T. E.* ~12 %). The decrease in ductility of the ***b*** processed condition tested in the (S-) direction can be explained by fracture along the flat grain boundaries of the large pancake shaped ***b*** grains which are oriented perpendicular to the S-loading direction.

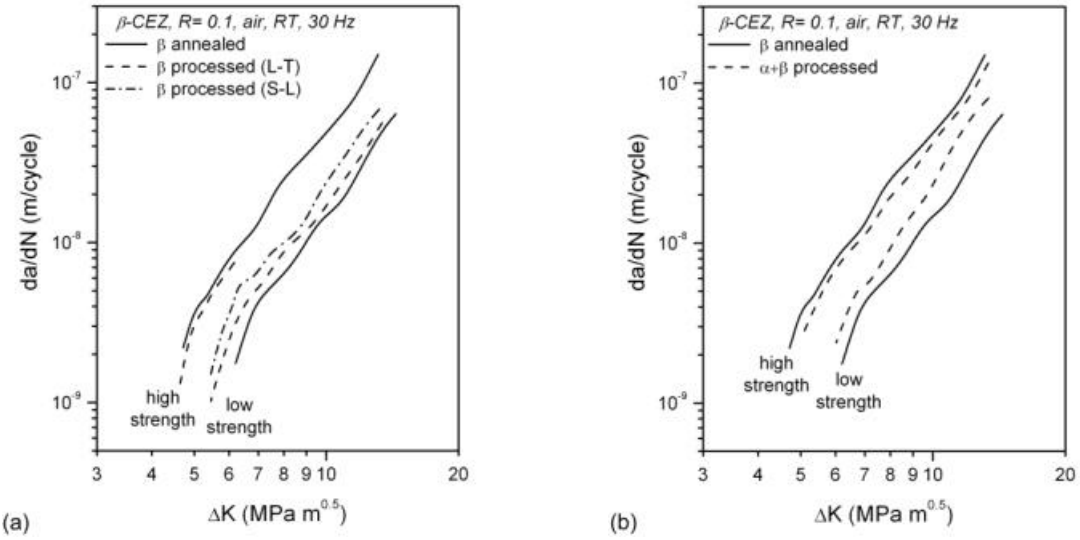

Figure 5. Fatigue crack growth curves. a) Comparison between *b* annealed and *b* processed microstructures, b) comparison between *b* annealed and *a* + *b* processed bimodal microstructures.

A comparison between crack growth rates of large cracks as a function of the applied stress intensity range of the ***b*** annealed and ***b*** processed conditions is shown in Fig. 5a, whereas Fig. 5b shows a comparison between ***b*** annealed and ***a*** + ***b*** processed conditions. Obviously, the three low strength conditions show a much higher fatigue crack growth threshold (~ $da/dN = 10^{-9}$ m/cycle) of $\Delta K_{TH} \sim 6$ MPa$\sqrt{m}$ as compared to $\Delta K_{TH} \sim 4$ MPa$\sqrt{m}$ measured for high strength conditions studied. Specifically at low strength level, the ***b*** annealed condition shows slightly higher fatigue crack growth resistance as compared to ***b*** processed (Fig. 5a) and ***a*** + ***b*** processed conditions (Fig. 5b). However, both high strength ***a*** + ***b*** processed and ***b*** processed conditions show

slightly higher crack growth resistance as compared to the β annealed condition. Typically for the class of β titanium alloys, microstructural variations with respect to size and shape of β grains were found not to impact the threshold behavior of large cracks, presumably due to the very small plastic zone size at the crack tip. Since the plastic zone at the crack tip is less than 2 µm for high and low strength conditions, it is clear that, as long as β grain boundaries are not aligned in the direction of crack extension, the size and shape of β grains have no influence on the fatigue crack growth threshold of large cracks.

Indeed, for the drastically different processed conditions of this study, crack front profiles in Figs. 6a to 12a show that large cracks propagate mainly through the lamellar matrix within the β grains. Since the high strength conditions exhibit a similar lamellar matrix the same threshold behavior resulted. The same tendency was found for the group of low strength conditions. On the contrary, testing the β processed condition in the S-direction resulted in lower threshold value (Fig. 5a) presumably because of high fractions of crack extension within soft zones along the flat grain boundaries of the large pancake shaped β grains which are oriented perpendicular to the S-loading direction (see Fig. 10a). Furthermore, based on data of low strength conditions, it can be assumed that testing of the β processed microstructure in high strength condition in S-direction would result in lowest threshold value measured in this study. However, since fatigue crack extension occurs mainly through the lamellar matrix within the β grains, it can be concluded that the resistance against fatigue crack growth is highly influenced by the coarse α plates affecting the crack front geometry. Consequently, comparison between the high and low strength conditions reveals the maximum effect of α plates on fatigue crack growth threshold. Thus, the maximum effect between the high and low strength conditions is a threshold difference of 2 MPa$\sqrt{m}$. In the fast crack propagation regime ($da/dN > 10^{-7}$ m/cycle) crack growth rates of studied microstructural conditions deviate from each other in accordance with the differences in K_{Ic} values as shown below.

Results of the fracture toughness testing are also shown in Table 1. For both strength levels, it can be seen that the β annealed and β processed conditions show ~30 % higher fracture toughness values as compared to the $\alpha + \beta$ processed conditions. Moreover, results of present study show, independently of microstructural condition, that fracture toughness values double as yield stress level decreased from 1500 MPa to 1050 MPa. To characterize the crack path at the onset of unstable crack advance, specimens were loaded up to corresponding fracture toughness values and immediately unloaded followed by heat tinting procedure to mark local crack fronts (as shown in detail in Ref. [1]). For both large grained β annealed and β processed conditions, it is obvious that the transition from fatigue precrack to initial unstable crack extension is characterized by pronounced grain boundary fracture, presumably due to the much larger plastic zone (~250 µm) ahead of the crack tip at high fracture toughness loads. Consequently, the plastic zone ahead of the crack tip, comparable to grain size dimensions, samples the microstructure for weak crack paths. Indeed, cracks tried to follow the soft zones along β grain boundaries in the β annealed and β processed conditions. The corresponding rough crack front profiles are shown in Figs. 6b and 8b (high strength), and 7b, 9b and 10b (low strength). For the β annealed conditions, it is found (based on marked heat tinted crack fronts) that the high strength condition shows ~90 % intergranular crack advance (Fig. 6b), whereas the low strength condition is characterized by lower fraction of grain boundary cracking (~75 %) and, consequently, a higher fraction of

transgranular fracture through the lamellar matrix. Whereas steps in the crack front of the high strength condition solely lead to crack advance along soft zones at the b grain boundaries, it is found that steps in the low strength condition preferentially result in a higher fraction of crack advance through the lamellar matrix. Due to the pancake grain shape of the b processed conditions the fracture surfaces are drastically different as compared to those of b annealed conditions. Since for the longitudinal (L-)direction the flat surfaces of the pancake shaped grains are parallel to the stress direction (L) and parallel to the transverse crack propagation direction (T), the fracture surface exhibit much lower fraction of grain boundary fracture (~30 % for the low strength, and ~50 % for the high strength condition) and fewer, but longer and higher steps, see crack front geometries in Figs. 8b (high strength) and 9b (low strength). Moreover, crack front profile is drastically different for testing in the longitudinal direction (Fig. 9b) as compared to the short transverse direction (Fig. 10b). For the S-direction, the flat surfaces of the pancake shaped grains are parallel to the crack plane and therefore the height of the steps is limited by the pancake thickness and the overall appearance of the nearly 100 % intergranular crack front profile is very flat (Fig. 10b). The crack front profiles of the $a+b$ processed conditions are very flat, due to the small b grain size (Figs. 11b and 12b). Apparently, the strength difference between the age hardened matrix and the soft zones along the continuous a layers at the b grain boundaries of the large grained b annealed or b processed high strength conditions is very high. Consequ-

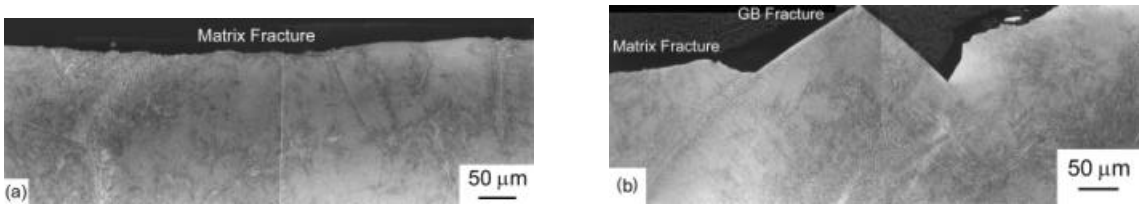

Fig. 6. *b* annealed high strength condition. Crack front profiles (LM) at a) low ΔK fatigue crack growth, and b) at onset of crack extension at K_{Ic} loading (crack path direction is normal to paper plane).

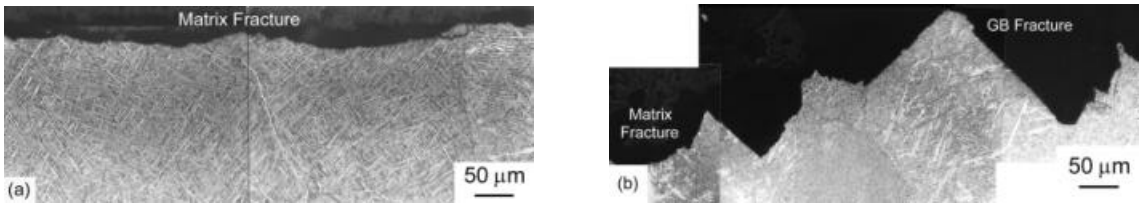

Fig. 7. *b* annealed low strength condition. Crack front profiles at a) low ΔK, and at K_c loading.

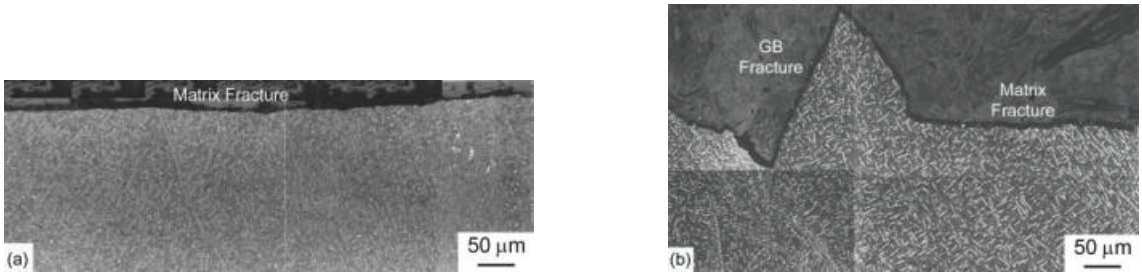

Fig. 8. *b* processed high strength condition (L-T). Crack front profiles at a) low ΔK , and b) K_{Ic} loading.

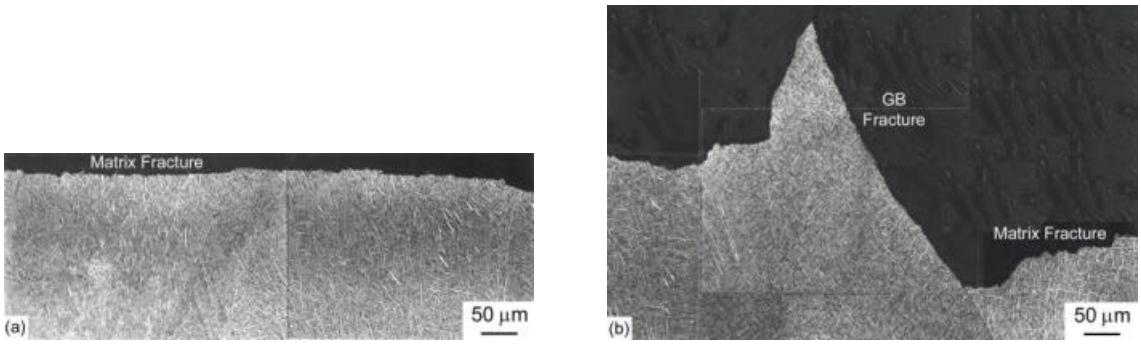

Fig. 9. *b* processed low strength condition (L-T). Crack front profiles at a) low ΔK , and b) K_c loading.

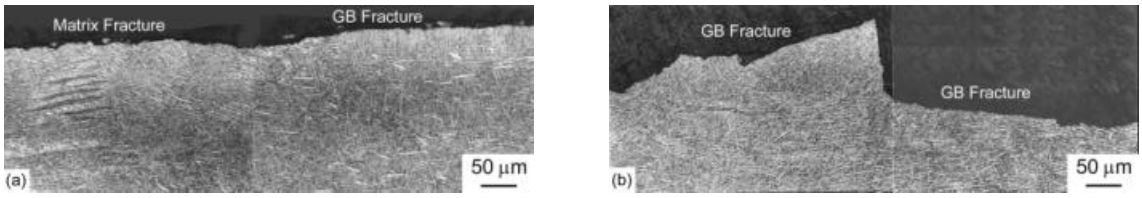

Fig. 10. *b* processed low strength condition (S-L). Crack front profiles at a) low ΔK , and b) K_c loading.

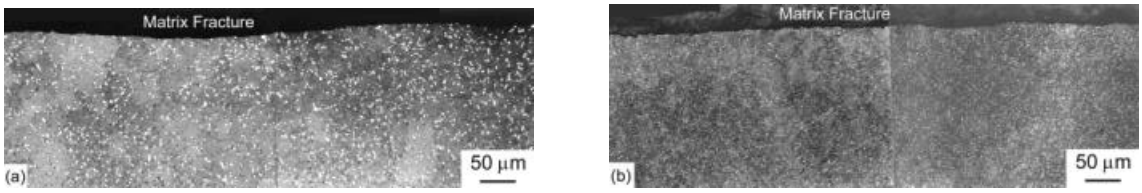

Fig. 11. *a* + *b* processed high strength condition. Crack front profiles at a) low ΔK , and b) K_{Ic} loading.

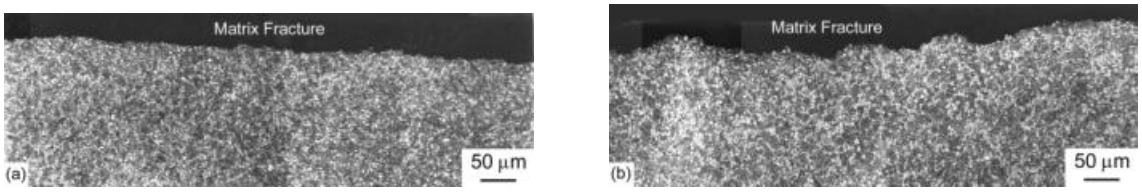

Fig. 12. *a* + *b* processed high strength condition. Crack front profiles at a) low ΔK , and b) K_c loading.

ently, the relatively low K_{Ic} values of 33 MPa√m (***b*** annealed) or 36 MPa√m (***b*** processed) can be attributed to the highly concentrated plastic deformation within the soft zones causing premature cracking before any measurable plastic deformation of the matrix occurs. The decreased strength level of the low strength conditions reduces the strength difference between the matrix and the soft zones to such a level that increased plastic deformation of the matrix can occur before fracture within the soft zones initiates. This is in general accordance with observed increasing tensile ductility measured in tensile test (Table 1). Therefore, part of the increase in fracture toughness from 33 and 36 MPa√m (high strength conditions) to 69 and 73 MPa√m (low strength conditions) can be attributed to the increase in plastic deformation of the lamellar matrix before onset of unstable crack advance occurs within the soft zones at the grain boundaries. But, as shown for the ***b*** annealed conditions by crack growth retarding steps in crack front geometry, the increase in the ductile transgranular fracture with decreasing stress level from 10 % (high strength condition) to 25 % (low strength

condition) also contributes to the observed increase in fracture toughness. For the β processed conditions, heat tinted fracture surfaces also reveal crack growth retarding effects of the long and high steps along grain boundaries preferentially aligned parallel to the stress direction (L) and parallel to the crack propagation direction (T). However, despite drastically differently oriented steps in the crack fronts of β annealed or β processed conditions, as well as much higher fraction of intergranular grain boundary fracture of the β annealed conditions, both microstructural conditions show nearly same fracture toughness values. The much lower fracture toughness values of the fine grained $\alpha + \beta$ processed conditions of 24 MPa√m (high strength) and 48 MPa√m (low strength condition) can be explained by very flat transgranular crack path, despite significant plastic deformation of the lamellar matrix before onset of unstable fracture (as shown by tensile tests). The lower fracture toughness for the β processed condition tested in S-direction (57 MPa√m (low strength condition)) as compared to L-testing direction (69 MPa√m) can be attributed to preferred crack extension within soft zones along the flat grain boundaries of the pancake shaped β grains. Obviously, crack growth retarding steps separating crack extension along flat grain boundaries of neighboring β grains are contributing to higher fracture toughness value as compared to $\alpha + \beta$ processed condition (48 MPa√m) with nominally flat crack path.

Reducing size and changing shape of β grains from β annealed large equiaxed to fine grained bimodal or to pancake shaped grain structures confirms crack path observations of a recent study [1] on β annealed large equiaxed grained microstructures. Principally, this study found that the crack growth retarding steps in the crack front effectively retard further propagation to form again a continuous crack front because the crack is forced to propagate along a microstructurally unfavored crack path and, moreover, under a very unfavorable angle with respect to the stress axis. Basically, the present study shows that the effective crack growth retarding mechanism of the steps in the crack front of the high strength β annealed or β processed conditions is solely based on unfavorable angle with respect to the stress axis, whereas steps in the low strength β annealed or β processed conditions effectively combine both mechanisms of microstructurally unfavored transgranular crack path through the lamellar matrix and an unfavorable angle with respect to the stress axis. For the $\alpha + \beta$ processed conditions, however, steps sizes are limited by small β grain size, and, therefore, are found to have no impact on crack growth resistance.

ACKNOWLEDGEMENTS

This work was supported by the Deutsche Forschungsgemeinschaft.

REFERENCES

1. Benedetti, M., Peters, J.O. and Lütjering, G. (2003) In: *Proceedings of the 10th World Conference on Titanium*, Lütjering, G. (Ed.), Wiley-VCH, Germany.
2. Peters, J.O. and Lütjering, G. (1998) *Z. Metallkd.* **89**, 464-473.
3. Sauer, C. and Lütjering, G. (2001) *Materials Science and Engineering* **A319-321**, 393-396.